2006

Absorption Properties of Dissolved and Particulate Matter in Turbid Productive Inland Lakes

Giorgio Dall'Olmo
Oregon State University, giorgiod@science.oregonstate.edu

Anatoly A. Gitelson
University of Nebraska - Lincoln, agitelson2@unl.edu

Dall'Olmo, Giorgio and Gitelson, Anatoly A., "Absorption Properties of Dissolved and Particulate Matter in Turbid Productive Inland Lakes" (2006). *Papers in Natural Resources*. 254.
https://digitalcommons.unl.edu/natrespapers/254

Dall'Olmo & Gitelson in Proceedings of Ocean Optics XVIII (Montreal, Quebec, October 9-13, 2006): 1-15.

Absorption Properties of Dissolved and Particulate Matter in Turbid Productive Inland Lakes

Giorgio Dall'Olmo[1] and Anatoly A. Gitelson[2]
1 – Dept. of Botany and Plant Pathology, Oregon State University, Corvallis, OR, 97331
2 – CALMIT-School of Natural Resources, University of Nebraska, Lincoln, NE 68588

INTRODUCTION

The absorption coefficient of natural waters, *a*, is defined as the fraction of monochromatic collimated light that is absorbed per unit of path length by an infinitesimally small volume of water (Preisendorfer, 1976). *a* depends on wavelength and is an inherent optical property, i.e. it depends exclusively on the characteristics of the optical medium and not on the geometric structure of the light field (Preisendorfer, 1976). Beside pure water itself, three other major constituents in the water column contribute to the absorption of solar energy: colored dissolved organic matter (subscript *CDOM*), suspended non-algal particles (subscript *nap*) and phytoplankton (subscript ϕ) (Mobley, 1994; Kirk, 1994).

Measurements of $a_{\phi}(\lambda)$ can be employed for estimating phytoplankton photosynthetic quantum yield (Kirk, 1994) and to extract information about the relative abundances of phytoplankton groups (Gege, 1995). On the other hand, measurements of $a_{CDOM}(\lambda)$ and $a_{nap}(\lambda)$ can be used to study the bio-physical characteristics of *CDOM* and non-algal particles (e.g. Yacobi et al., 2003; Babin and Stramski, 2004), as well as to analyze the spectral distribution and the intensity of the light available to phytoplankton. Furthermore, the spectral total absorption coefficient is one of the main factors that determines heating of the water column (Kirk, 1988; Morel and Antoine, 1994) with strong bio-physical implications for the aquatic ecosystem. Finally, most remote sensing algorithms require knowledge of the relative contributions of the different constituents to the total absorption coefficient as a function of wavelength (Gons, 1999; Dall'Olmo and Gitelson, 2005).

The absorption properties of oceanic waters have been extensively analyzed (e.g. Gordon and Morel, 1983; Kirk, 1994) and detailed studies on the absorption coefficients of coastal and estuarine regions have been recently presented (Babin et al., 2003; Magnuson et al., 2004; Gallegos, 2005; Gallegos et al., 2005; Doxaran et al., 2006). However, turbid productive inland lakes have received less attention despite their importance as freshwater supplies and recreational areas. Optical properties of lakes may provide for example the time series of data needed to understand and predict the occurrence of toxic cyanobacterial blooms.

a_{CDOM} is the most common absorption measurement carried out in turbid productive lakes with values at 440 nm ranging widely from 0.06 to 20 m^{-1} (Kirk, 1994). Similarly, published values of total particle absorption coefficients ($a_{nap}+a_{\phi}$) display large variances (Davies-Colley, 1983; Kirk and Tyler, 1986; Bowling et al., 1986; Oliver, 1990; Alvarez-Cobelas, 1991). These large variations suggest that absorption coefficients measured directly or obtained by inverting reflectance spectra have a strong potential for characterizing turbid productive lentic ecosystems.

Measurements of a_{ϕ} and a_{nap} in turbid productive inland waters are more limited. Most published data have been collected from European lakes (Dekker et al., 1997; Duarte et al., 2000; Pierson and Strömbäck, 2000; Kutser et al., 2001; Simis et al., 2005; Reinart et al., 2005), although oligotrophic and mesotrophic lakes in North America have been investigated (Bukata et al., 1979; Weidemann *et al.*, 1985; Weidemann & Bannister, 1986; Bergmann et al., 2004).

The objective of this study is to extend the knowledge on the absorption properties of turbid productive lakes by describing the spectral characteristics of a_{CDOM}, a_{nap} and a_{ϕ} spectra measured in an agriculturally dominated region of North America (Nebraska, USA).

STUDY AREA

Data were collected in eastern Nebraska during 2002 and 2003 (from May through October) from the sand-pit lakes of Fremont (#1, #2, #3, #5, #12; Lat. 41.4426, Long. 96.5651) from Ginger Cove (Lat. 41.3120, Long=-96.3594), and from the Branched Oak reservoir (Lat. 40.9714, Long= -96.8654). Additional samples were collected from April through October 2005 from sand pit lakes (Benak 8, Benak 8a, Copper Dollar Cove, Cedar Creek Lake) located near Plattsmouth, NE (Lat. 40.9880, Long=- 95.9880) and from the Fremont State Lakes #1, #3, #5 and #20. The sampling locations were chosen to cover an as wide as possible range of optical conditions. The sampled water bodies are relatively shallow (in average they range between 3-15 m), with relatively small surface areas (10-600 ha). A total of more than 300 absorption spectra and relevant water constituents were measured.

METHODOLOGY

Ancillary measurements – Chlorophyll-a concentration (Chl) was measured fluorometrically (Welschmeyer, 1994) after extracting in 96% hot ethanol samples that were gently filtered on GF/F Whatman filters. The absorbance of the pure chlorophyll-a (Sigma) solution that was used as the standard for the fluorometer was measured in a Cary 100 Varian spectrophotometer from 400 to 750 nm. Fluorometric measurements were first normalized to the absorbance at 665 nm of the standard. Subsequently, these intercalibrated fluorometric measurements were converted into chlorophyll-a concentrations by applying a calibration coefficient. This calibration coefficient was obtained, for a limited set of samples, from a regression between normalized fluorometric measurements and concurrent High-Performace Liquid Chromatography chlorophyll-a concentrations carried out by Laurie Van Heukelem at Horn Point Laboratory, Univ. of Maryland.
Total and inorganic suspended solids, *TSS* and *ISS* respectively, were measured gravimetrically after collection on GF/F Whatman filters (American Public Health Association, 1989).

Colored Dissolved Organic Matter absorption (a_{CDOM}) – Water samples were filtered through Whatman GF/F filters (nominal pore size 0.7 μm) before spectrophotometric absorbance measurements. Samples collected during 2003 and 2005 were additionally filtered through Whatman 0.2 μm nylon membrane filters. Absorbance measurements (from 400 to 800 nm) were carried out using a double-beam Varian Cary 100 spectrophotometer equipped with 10 cm path length quartz cuvettes. Baselines were automatically subtracted from each sample measurement. Optical density (*OD*) was converted to absorption coefficient (*a*) as: $a(\lambda) = \frac{\ln(10)\left(OD - \langle OD(782)\rangle\right)}{x}$; where *x* is the path length (in meters) and $\langle OD(782)\rangle$ is the median value of *OD* between 780 and 784 nm which was subtracted to remove potential scattering interferences. This procedure assumes that scattering errors are spectrally flat, also know as "null-point correction". The spectral range 780-784 nm was chosen because it is minimally affected by temperature-dependent variations in water absorption (Buiteveld et al., 1994) and $a_{CDOM}(782)$ is expected to be negligible in the lakes we sampled. Spectra contaminated by *Chl* were identified as those for which $a_{CDOM}(676) \geq a_{CDOM}(655)$ and removed from the rest of the analysis.

To statistically describe the data, a_{CDOM} spectra were then fitted, from 400 to 550 nm, using a Levemberg-Marquard non-linear routine to the exponential model (Bricaud et al., 1981) $a_{CDOM}(\lambda) = a_{CDOM}(440)\exp[-S_{CDOM}(\lambda - 440)]$; where S_{CDOM} is the spectral slope of a_{CDOM}.

Total particle absorption (a_p) – Following the procedure described by Fargion & Mueller (2000), the absorption coefficient of total suspended particles was calculated from spectrophotometric absorbance measurements. Suspended particles were collected onto filters (Whatman, GF/F) by gentle filtration and scanned from 400 to 800 nm in the Cary 100 spectrophotometer against a clean wet (Milli-Q) reference filter. The instrument baseline was automatically subtracted from each sample measurement. Sample and reference filters were kept wet during the entire measurement time. We note that the filters were not in direct contact with the detector, nor was a diffuser placed between filter and detector. Thus, inaccuracies in the absorption coefficients are expected because a fraction of the light transmitted through the filter is lost due to scattering. After correction for this scattering error (see below), the absorption coefficient was then calculated as:

$$a(\lambda) = \ln(10) OD_s(\lambda) \frac{S}{V} \qquad (1)$$

where OD_s is the optical density of a suspension with a geometric path length equal to that of the particles on the filter, S is the clearance area of the filter (in m^2) and V is the volume of water filtered (in m^3). The calculation of OD_s is presented in detail below.

Non-algal particle absorption (a_{nap}) – After total particle absorption measurements, filters were bleached with chlorine water solution (0.2%) to remove phytoplankton pigments (Tassan and Ferrari, 1995). Each filter was reinstalled on the filtration rack and pre-bleached by gently adding 5 ml of chlorine solution on the filter. After approximately 5 minutes the residual chlorine was removed and an additional 10 ml of chlorine solution were added. After approximately 10-15 minutes, the sample was rinsed with 20-40 ml of MilliQ water and its absorbance measured in the spectrophotometer against a clean filter that was processed in the same way. After correction for scattering error (see below), a_{nap} was computed using Eq. (1). To statistically describe the data, a_{nap} spectra were fitted (using a Levemberg-Marquard non-linear routine), from 400 to 550 nm, to the exponential model (Babin et al., 2003) $a_{nap}(\lambda) = a_{nap}(443)\exp[-S_{nap}(\lambda - 443)]$;where S_{nap} is the spectral slope of a_{nap}.

Spectra contaminated by *Chl* were identified as those spectra for which $a_{nap}(676) \geq a_{nap}(655)$ and removed from the analysis.

Phytoplankton pigment absorption (a_ϕ) – The absorption coefficient of phytoplankton cells was finally computed by subtracting a_{nap} from a_p: $a_\phi = a_p - a_{nap}$.

β factor – The path-length amplification factor β links the optical density of samples on filters (OD_f) and the optical density of samples in suspensions (OD_s); it accounts for the increase in path length of

photons in the filter (due to scattering by the glass fibers) with respect to the suspension. It is without doubt the most important source of uncertainty in the quantitative filter technique (e.g. Finkel and Irwin, 2001). Because of the variability of the values reported in the literature, experiments were carried out to quantify β following the empirical methodology proposed by Butler (1962). Water samples were collected from the Fremont State Lakes (on 07/13/05 and 08/03/05), Branched Oak reservoir (on 07/14/05) and concentrated by centrifugation. Additional samples were obtained by using dense cultures of *Microcystis* and *Synechococcus* which were grown in the Limnology Laboratory, University of Nebraska-Lincoln. A total of 15 spectra were used for the analysis, among which 10 were from natural samples and 5 from algal cultures.

Optical densities of samples in suspension, OD_s, were measured in a Shimadzu 2501-PC double-beam spectrophotometer equipped with a 6-cm integrating sphere. 1-cm quartz cuvettes were positioned in contact with the entrance ports of the sphere. The baseline of the instrument was automatically corrected by measuring, at the beginning of each experiment, sample water filtered through Whatman 0.2 μm nylon membrane filters. Measurements were collected in absorbance mode from 400 to 800 nm, with a spectral sampling interval of 1 nm. Residual scattering errors were removed as described in the *"Residual scattering error"* section.

Optical densities of samples on filters, OD_f were measured in the Variant Cary 100 double-beam spectrophotometer from 400 to 800 nm, in absorbance mode with a sampling interval of 1 nm. Baselines were measured at the beginning of each experiment by scanning two pre-wetted (with approximately 250 ml of MilliQ water) Whatman GF/F filters; baselines were then automatically subtracted from subsequent sample measurements. Particles were collected on GF/F filters by gentle filtration. By adjusting the volumes of water filtered, the path lengths of the samples on filters were kept equal to the path lengths of the corresponding samples in suspension. Residual scattering errors were removed as described in the *"Residual scattering error"* section.

The β-factor correction, i.e. the relationship linking optical density on filters (OD_f) and in suspension (OD_s), was obtained by non-linear (Levemberg-Marquart) fit of the experimental optical density measurements to $OD_s = p_1 OD_f^{\,p_2}$; where p_1=0.7348±0.0070 and p_2=1.2721±0.0074, the number of points used for the regression was 6015 and the determination coefficient r^2=0.953.

Residual scattering error – Typically it is assumed that the scattering error in filter-pad measurements is spectrally independent and its influence is removed from the absorption spectrum by subtracting the (apparent) absorption measured at a wavelength in the near-infrared (i.e. 750-800 nm). The additional underlying assumption is that in such spectral region, absorption by particles is negligible and thus any detectable signal is related to scattering. However, when such methodology is applied to our data set, there appears to be a residual scattering (or apparent absorption) contamination that is likely due to a spectral dependence of the scattering error. For example, the inset of Figure 1a shows that after subtraction of $a_{nap}(800)$ from the entire spectrum, absorption at wavelengths higher than 750 nm is not negligible. This may imply that either there is a significant absorption in the NIR spectral region, or, most likely, that the scattering error is spectrally dependent. Therefore, an alternative method was devised to remove this scattering error.

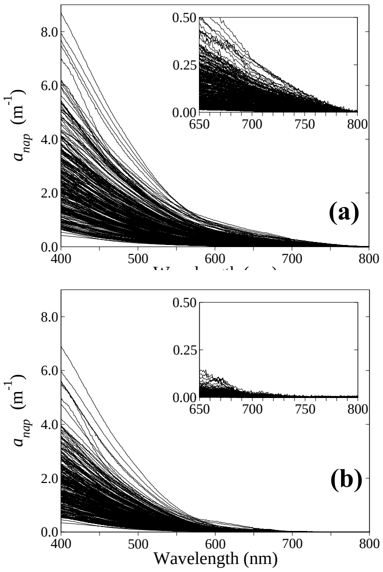

Figure 1 – (a) Non-algal particle absorption spectra corrected for the scattering error by subtracting a_{nap}(800). The inset represents the red-NIR spectral region in greater detail. (b) Non-algal particle absorption spectra corrected for the scattering error by subtracting from each spectrum a straight line that was fitted from 750 to 800 nm. The inset represents the red-NIR spectral region in greater detail.

Under the assumption that the scattering error is linearly dependent on wavelength, a straight line was fitted to each absorption spectrum from 750 to 800 nm. This straight line represents the scattering error and was then subtracted from the entire OD_f spectrum. The result of the two different methods for correcting the scattering error are exemplified in Figure 1 for the a_{nap} spectra, showing that subtraction of the linear fit reduces the absorption signal in the NIR considerably more than the simple subtraction of a_{nap}(800). This linear scattering error subtraction was applied to both the total particle and the non-algal particle absorption spectra. The assumption of a linear dependence of the scattering error is expected to be appropriate for the red-NIR spectral region, but it probably causes an underestimation of the scattering error in the blue-green spectral region. Finally, we recognize that there are studies suggesting that particle absorption in the NIR may not be negligible (Tassan and Ferrari, 2003); however, because this issue is still open, we considered a_{nap} negligible in the 750-800 nm region.

RESULTS AND DISCUSSION

Chl and *TSS* – The lakes sampled were indeed turbid and productive with median *Chl* around 29 mg m^{-3} and median *TSS* around 12 g m^{-3} (Figure 2). Notably, in the Fremont State Lakes (FSL) #1, #2, #3, #5, and #12 and in the Branched Oak reservoir (BO) that were measured in 2002 as well as 2003, *Chl* was considerably higher in the former than in the latter year with median values of 67 and 25 mg m^{-3}, respectively (Figure 2).

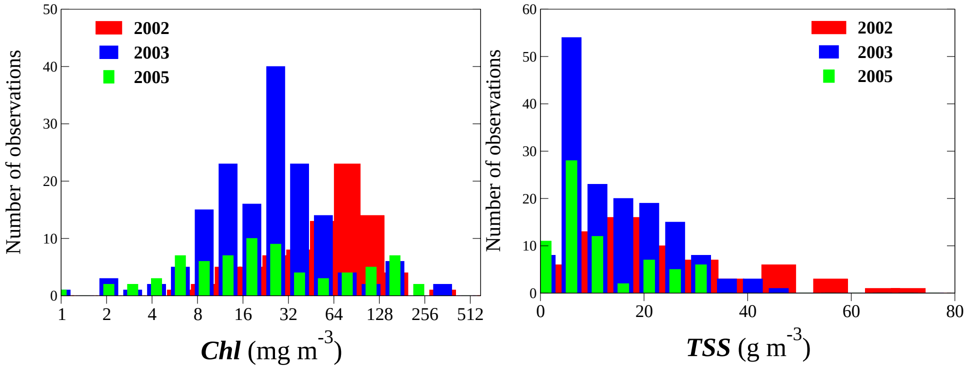

Figure 2 – Histograms of Chl and TSS. Note the logarithmic scale for the Chl axis.

Absorption coefficient of colored dissolved organic material – The spectral slope of CDOM, S_{CDOM}, differed between samples collected in 2002 and samples collected in 2003 and 2005 (Figure 3a) despite the coincidence in sampling locations during 2002 and 2003. a_{CDOM} spectra measured in 2002 from 0.7-µm filtered samples showed lower S_{CDOM} values (median=0.0133 nm^{-1}) than spectra measured in 2003 and 2005 from 0.2-µm filtered samples (medians 0.0168 and 00169 nm^{-1}, respectively).

To provide a reference for the current absorption measurements, we compared our inland water observations to the extensive data set assembled for European coastal waters by Babin et al. (2003). The S_{CDOM} values measured in 2003 and 2005 compared favorably to the S_{CDOM} statistics obtained from spectra measured from European coastal water samples filtered on 0.2-µm filters (Babin et al, 2003). The slight overestimation of the median S_{CDOM} value (0.0168 nm^{-1} in Nebraska vs. 0.0176 nm^{-1} in European costal waters) can be attributed entirely to the wavelength used for the null-point scattering correction which was set at 685 nm in Babin et al., 2003. When we used the same wavelength for the null-point scattering correction median S_{CDOM} values for Nebraska lakes increased to about 0.018 nm^{-1} (Figure 3b).

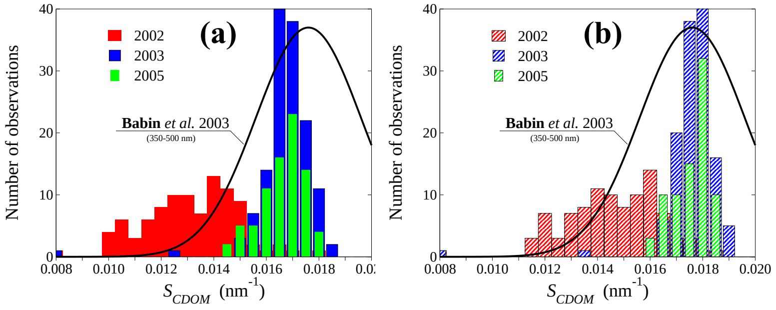

Figure 3 – (a) Frequency distribution of the S_{CDOM} obtained by fitting a_{CDOM} spectra from 400 to 550 nm after a null-point scattering correction using raw optical density values at 782 nm. (b) The null-point scattering correction was carried out using raw optical density values at 685 nm. The black curve corresponds to the statistics presented by Babin et al. (2003) for European coastal waters and obtained by fitting a_{CDOM} spectra from 350 and 500 nm.

Figure 4 demonstrates that in Nebraska lakes $a_{\text{CDOM}}(440)$ ranged from 0.2 to 2.0 m^{-1} during 2003 and 2005, and from approximately 0.5 to 2.5 m^{-1} in 2002. Therefore, the magnitude of absorption was higher in the inland lakes sampled, even though in 2003 and 2005 the S_{CDOM} values were comparable to those measured in European coastal waters.

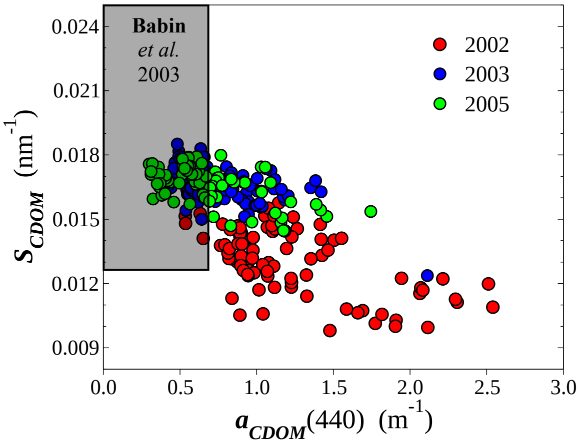

Figure 4 – Scatter plot between S_{CDOM} and a_{CDOM}(440). The shaded rectangle represents approximately the range of values found in European coastal waters (Babin et al., 2003).

We also investigated the differences in S_{CDOM} and a_{CDOM}(440) from samples collected from the same lakes in 2002 and 2003. a_{CDOM} spectra collected in 2002 showed lower S_{CDOM} and higher a_{CDOM}(440) than in 2003 suggesting that the 0.7-μm filters used in 2002 allowed a larger number of particles/molecules to pass through the filters. This larger number of absorbing particles was likely responsible for the larger a_{CDOM}(440) values found in 2002. The 0.7-mm filtered sampled also included particles with larger sizes, which is consistent with lower values on S_{CDOM} in 2002 than in 2003 (Hayase and Tsubota, 1985; Summers et al., 1987; Carder et al., 1989; Pages and Gadel, 1990; Yacobi et al., 2003). To examine the influence of productivity on the spectral properties of CDOM we plotted S_{CDOM} and a_{CDOM}(440) as a function of *Chl* and *TSS* (Figure 5). We found that the difference in S_{CDOM} and a_{CDOM}(440) between the two years was independent of either *Chl* and *TSS*. Thus we concluded that a significant fraction of absorbing material might have been characterized by size ranging from 0.2 to 0.7 μm.

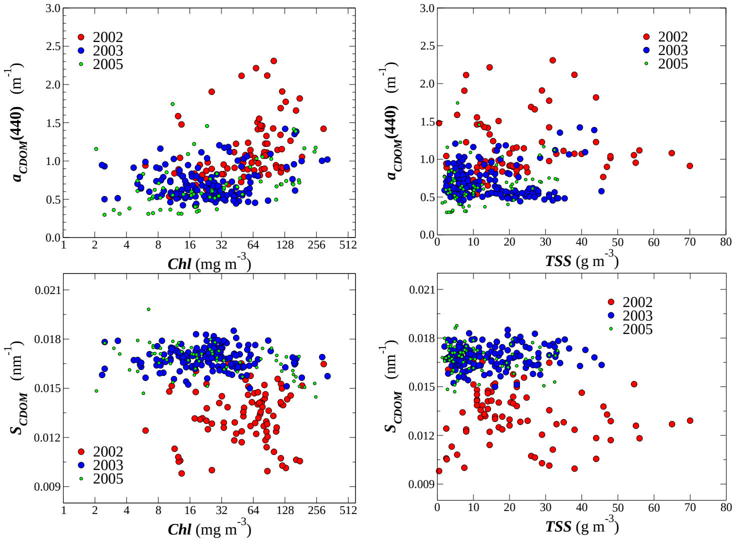

Figure 5 – Scatter plots between CDOM absorption properties and Chl and TSS. Note the logarithmic scale for the Chl axes.

Figure 6 shows that S_{CDOM} was inversely related to $a_{\mathrm{CDOM}}(440)$. Since S_{CDOM} has been found to be roughly inversely related to the molecular weight of CDOM (Hayase and Tsubota, 1985; Summers et al., 1987; Carder et al., 1989; Pages and Gadel, 1990; Yacobi et al., 2003), data of Figure 7 could be related to the process of decomposition of large molecules of humic substances into smaller ones. As this process advances, the concentration of CDOM decreases, as does a_{CDOM}. Thus, the relationships found between S_{CDOM} and $a_{CDOM}(440)$ may indicate that, it could be possible to follow the mineralization of CDOM by measuring the spectral characteristics of the absorption coefficient of CDOM. Moreover, significant S_{CDOM}–$a_{CDOM}(440)$ relationships may indicate that, during 2003 in a certain lake, dissolved organic matter had a common origin and that it underwent similar degradation processes. On the other hand, weak relationships between S_{CDOM} and $a_{CDOM}(440)$ may indicate that CDOM had different sources or degradation pathways in 2003. In addition we noted that as the bio-mineralization process advanced, S_{CDOM} increased to a value (about 0.018 nm^{-1}) that was approximately constant among different lakes (Figure 6). This maximal S_{CDOM} value may correspond to the minimal molecular weight detectable using optical measurements in the visible spectrum. On the other hand, the approximately constant $a_{CDOM}(440)$ value (0.5 m^{-1}) found in correspondence of the maximal S_{CDOM} does not seem to be related to any bio-physical mineralization process. This is because it seems unlikely that the mineralization of different amounts of CDOM leads, in different water bodies, to the same minimal concentration of CDOM. Thus, we suspect that an unexplained systematic bias may be affecting our a_{CDOM} spectra. More studies are required to clarify this issue.

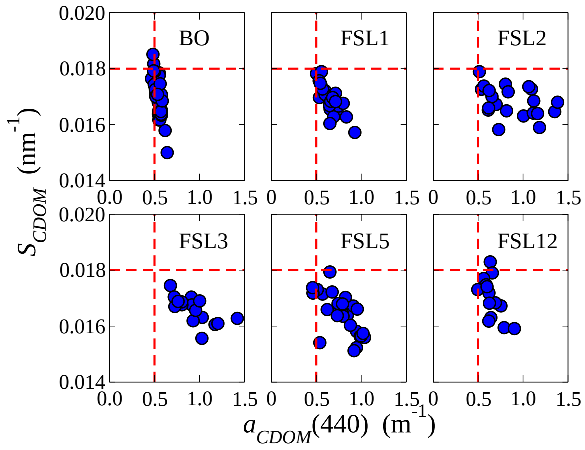

Figure 6 – Scatter plots between S_{CDOM} and $a_{CDOM}(440)$ for separate lakes in 2003. The horizontal dashed lines are set at S_{CDOM} =0.018 nm^{-1}; the vertical dashed lines are set at $a_{CDOM}(440)$=0.5 m^{-1}.

Absorption coefficient of non-algal particles – The spectral slope of the non-algal particle component, S_{nap}, was rather independent of time and place of sampling and it ranged between 0.008 and 0.018 nm^{-1} (median value 0.0122 nm^{-1}), in agreement with European coastal waters (Figure 7).

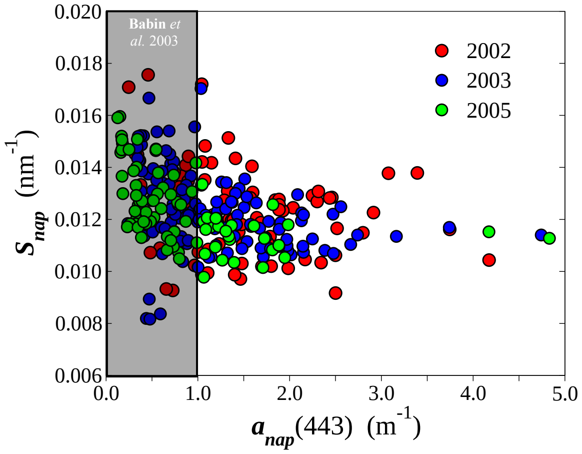

Figure 7 – Scatter plot between S_{nap} and a_{nap}(443). The shaded area approximately corresponds to the range of values found in European coastal waters by Babin et al. (2003).

On the other hand, the magnitude of the non-algal particle absorption at 443 nm ranged from 0.2 to 5.0 m^{-1}, thus being as much as three times as high as the values reported by Babin et al. (2003).

a_{nap}(443) covaried with *TSS* (data not shown), but the slope of such relationship, the ratio $a^*_{nap}(443)=a_{nap}(443)/TSS$, was higher (median value 0.074 m^2 g^{-1}) than that found for European coastal waters (0.041 m^2 g^{-1}, Figure 8). Such a discrepancy is not surprising given the dependency of a^*_{nap} on the refractive index of particles and their size distribution (Mikkelsen, 2002). In an attempt to explain at least part of the observed difference, we arbitrarily grouped our samples as samples characterized by an inorganic fraction (*ISS*/*TSS*) greater than 50%, and lower than 50%. The first group included mostly particles of mineral origin (less absorbing), while the second mostly particle of organic origin (more absorbing). As expected the observed median values of a^*_{nap} was lower (0.055 m^2 g^{-1}) for the more mineral group, and higher (0.076 m^2 g^{-1}) for the group containing more organic particles. Finally, we note that a^*_{nap} was obtained by normalizing a_{nap} by the concentration of total suspended solids, *TSS*, that included both phytoplanktonic and non-phytoplanktonic particles. Thus, we expect our estimates of a^*_{nap} to be lower than their true values due to the contribution of algal biomass to *TSS*.

Dall'Olmo & Gitelson in Proceedings of Ocean Optics XVIII (Montreal, Quebec, October 9-13, 2006): 1-15.

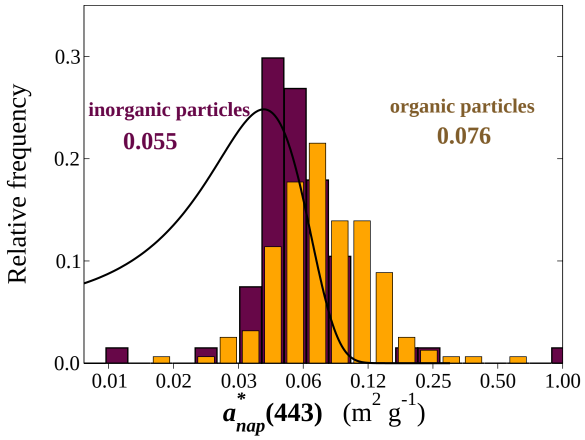

Figure 8 – Frequency distributions of $a^*_{nap}(443)$ by particles mostly of inorganic origin (ISS/TSS>0.5) and mostly of organic origin (ISS/TSS<0.5). The black line represents the statistics obtained by Babin et al. (2003) for European coastal waters (average $a^*_{nap}(443)=0.041\ m^2\ g^{-1}$).

Absorption coefficient of phytoplankton pigments – All the measured phytoplankton absorption spectra, normalized by their corresponding *Chl* are presented in Figure 9. a^*_ϕ displayed a large range of variability in the blue spectral region due to variations in ancillary pigments and packaging effect.

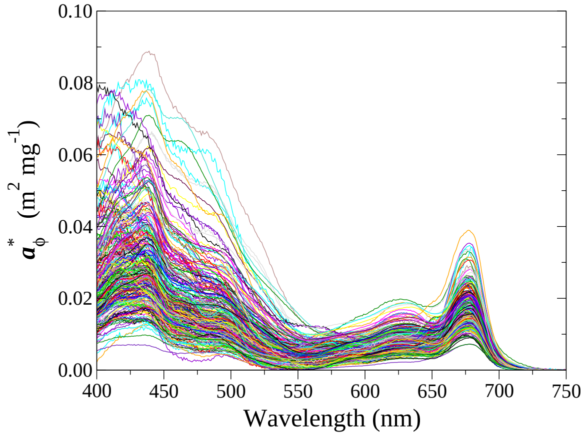

Figure 9 – Chl-specific phytoplankton absorption spectra.

The examples of *Chl*-specific absorption spectra presented in Figure 10 show the great variability of ancillary pigments that characterized the different phytoplankton groups sampled. Phycobilins carrying Cyanophyta and Cryptophyta show local peaks of absorption around 625 nm (phycocyanin) and 570 nm (phycoerythrin), respectively. Chlorophyta displayed the signature of chlorophyll-b with local absorption peaks in-vivo around 480 and 650 nm.

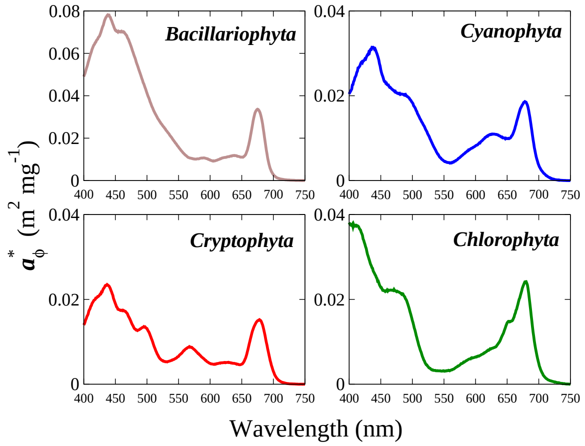

Figure 10 – Examples of Chl-specific phytoplankton spectra dominated by characteristic algal taxa (as determined by microscopy).

The magnitude of $a^*_\phi(676)$ ranged between 0.009 and 0.038 m^2 mg^{-1} with median values at 0.0156 m^2 mg^{-1} and was only weakly correlated with *Chl* (Figure 11).

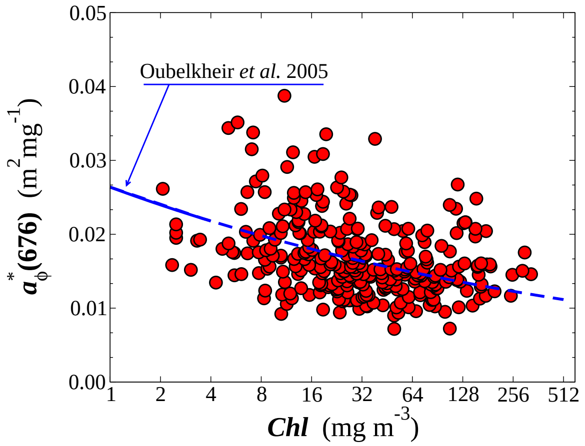

Figure 11 – Scatter plot between $a^*_\phi(676)$ and Chl. The blue line represents the fit derived by Oubelkheir et al. (2005) (the dashed part of the curve is the extrapolation to our Chl range).

CONCLUSIONS

We have presented an extensive dataset on the absorption properties of dissolved and suspended particles of ten productive Nebraska lakes. The spectral slopes of the non-algal particles and CDOM absorption coefficients, as well as the *Chl*-specific phytoplankton absorption at 676 nm agreed well with those reported for European coastal and open Mediterranean waters despite the clear differences in the trophic states of these very different types of water bodies. On the other hand, the high productivity of the lakes sampled was evident in the observed magnitudes of a_{CDOM}, a_{nap} and a_{ϕ} that were all considerably higher that those reported for European coastal waters. Another important peculiarity of the inland waters studied was the high $a^{*}_{nap}(443)$ coefficient which indicated a high fraction of organic matter in suspension and/or small particle sizes. Finally, this study raised a question regarding the importance of the absorbing material with sizes included in the 0.2 to 0.7 μm range.

REFERENCES

Alvarez-Cobelas, M. (1991). Optical Limnology of a Hypertrophic Gravel-Pit Lake. *Internationale Revue Der Gesamten Hydrobiologie*, *76*(2)*,* 213-223.

Babin, M., Stramski, D., Ferrari, G.M., Claustre, H., Bricaud, A., Obolensky, G. & Hoepffner, N. (2003). Variations in the light absorption coefficients of phytoplankton, nonalgal particles, and dissolved organic matter in coastal waters around Europe. *Journal of Geophysical Research-Oceans*, *108*(C7)*,* 3211, doi:10.1029/2001JC000882.

Babin, M. & Stramski, D. (2004). Variations in the Mass-Specific Absorption Coefficient of Mineral Particles Suspended in Water. *Limnology and Oceanography*, *49*(3)*,* 756-767.

Bricaud, A., Morel, A. & Prieur, L. (1981). Absorption by dissolved organic matter of the sea (yellow substance) in the UV and visible domains. *Limnology and Oceanography* , *1,* 43-53.

Buiteveld, H., Hakvoort, J.H.M., and Donze, M.(1994). The optical properties of pure water. *Ocean Optics XII,* Bergen, Norway.

Bukata, R.P., Jerome, J.H., Bruton, J.E. & Jain, S.C. (1979). Determination of inherent optical properties of Lake Ontario coastal waters. *Applied Optics*, *18*(23)*,* 3926-3932.

Bowling, L.C., Steane, M.C. & Tyler, P.A. (1986). The spectral distribution and attenuation of underwater irradiance in Tasmanian inland waters. *Freshwater Biology*, *16,* 313-335.

Bergmann, T., Fahnenstiel, G., Lohrenz, S., Millie, D. & Schofield, O. (2004). Impacts of a recurrent resuspension event and variable phytoplankton community composition on remote sensing reflectance. *Journal of Geophysical Research C: Oceans* , *109*(C10S15)*,* doi:10.1029/2002JC001575.

Bukata, R.P., Jerome, J.H., Bruton, J.E., Jain, S.C. & Zwick, H.H. (1981). Optical water quality model of Lake Ontario. 1:Determination of the optical cross sections of organic and inorganic particulates in Lake Ontario. *Applied Optics*, *20*(9)*,* 1696-1703.

Butler, W.L. (1962). Absorption of light by turbid materials. *Journal of the Optical Society of America*, *52,* 292-299.

Carder, K.L., Steward, R.G., Harvey, G.R. & Ortner, P.B. (1989). Marine humic and fulvic acids: their effects on remote sensing of ocean chlorophyll. *Limnology & Oceanography*, *34*(1)*,* 68-81.

Dall'Olmo, G. & Gitelson, A.A. (2005). Effect of bio-optical parameter variability on the remote estimation of chlorophyll-a concentration in turbid productive waters: experimental results. *Applied Optics*, *44*(3) *,* 412-422.

Davies-Colley, R.J. (1983). Optical properties and reflectance spectra of 3 shallow lakes obtained from a spectrophotometric study (Waikato Basin). *New Zealand Journal of Marine & Freshwater Research*, *17*(4)*,* 445-459.

Dekker, A.G., Hoogenboom, H.J., Goddijn, L.M. & Malthus, T.J.M. (1997). The relation between inherent optical properties and reflectance spectra in turbid inland waters. *Remote Sensing Reviews*, *15*(1-4)*,* 59-74.

Doxaran, D., Cherukuru, N. & Lavender, S. (2006). Apparent and inherent optical properties of turbid estuarine waters: measurements, empirical quantification relationships and modelling. *Applied Optics*, *45*(10)*,* 2310-2324.

Duarte, C.M., Agusti, S. & Kalff, J. (2000). Particulate Light Absorption and the Prediction of Phytoplankton Biomass and Planktonic Metabolism in Northeastern Spanish Aquatic Ecosystems. *Canadian Journal of Fisheries and Aquatic Sciences*, *57*(1)*,* 25-33.

Fargion, G. S. and Mueller, J. L.(2000). *Ocean optics protocols for SeaWiFS validation, Revision 2*. Greenbelt, Maryland: NASA Goddard Space Flight Center. pp. 184.

Finkel, Z.V. & Irwin, A.J. (2001). Light Absorption by Phytoplankton and the Filter Amplification Correction: Cell Size and Species Effects. *Journal of Experimental Marine Biology and Ecology*, *259*(1) *,* 51-61.

Gallegos, C.L. (2005). Optical Water Quality of a Blackwater River Estuary: the Lower St. Johns River, Florida, Usa. *Estuarine Coastal and Shelf Science*, *63*(1-2)*,* 57-72.

Gallegos, C.L., Jordan, T.E., Hines, A.H. & Weller, D.E. (2005). Temporal Variability of Optical Properties in a Shallow, Eutrophic Estuary: Seasonal and Interannual Variability. *Estuarine Coastal and Shelf Science*, *64*(2-3)*,* 156-170.

Gons, H.J. (1999). Optical teledetection of chlorophyll a in turbid inland waters. *Environmental Science & Technology*, *33*(7)*,* 1127-1132.

Gordon, H.R. & Morel, A. (1983). *Remote assessment of ocean color for interpretation of satellite visible imagery. A review*. New York: Springer-Verlag.

Hayase, K. & Tsubota, H. (1985). Sedimentary humic acid and fulvic acid as fluorescent organic materials. *Geochimica et Cosmochimica Acta*, *49*(1)*,* 159-163.

Jupp, D.L.B., Kirk, J.T.O. & Harris, G.P. (1994). Detection, Identification and Mapping of Cyanobacteria - Using Remote-Sensing to Measure the Optical-Quality of Turbid Inland Waters. *Australian Journal of Marine and Freshwater Research*, *45*(5)*,* 801-828.

Kirk, J.T.O. (1988). Solar heating of water bodies as influenced by their inherent optical properties. *Journal of Geophysical Research* , *93*(D9)*,* 10,897-10,908.

Kirk, J.T.O. & Tyler, P.A. (1986). The spectral absorption and scattering properties of dissolved and particulate components in relation to the underwater light field of some tropical Australian freshwaters. *Freshwater Biology*, *16,* 573-583.

Kirk, J.T.O. (1994). *Light and photosynthesis in aquatic ecosystems*. Cambridge, United Kingdom: Cambridge University Press. pp. 509.

Kutser, T., Herlevi, A., Kallio, K. & Arst, H. (2001). A Hyperspectral Model for Interpretation of Passive Optical Remote Sensing Data From Turbid Lakes. *Science of the Total Environment*, *268*(1-3)*,* 47-58.

Magnuson, A., Harding, L.W., Mallonee, M.E. & Adolf, J.E. (2004). Bio-Optical Model for Chesapeake Bay and the Middle Atlantic Bight. *Estuarine Coastal and Shelf Science*, *61*(3)*,* 403-424.

Mikkelsen, O.A. (2002). Variation in the projected surface area of suspended particles: Implications for remote sensing assessment of TSM. *Remote Sensing of Environment*,(1)*,* 23-29.

Mobley, C.D. (1994). *Light and water: radiative transfer in natural waters*. San Diego, CA: Academic Press. pp. 592.

Morel, A. & Antoine, D. (1994). Heating rate within the upper ocean in relation to its bio-optical state. *Journal of Physical Oceanography*, *24*(7)*,* 1652-1665.

Oliver, R.L. (1990). Optical Properties of Waters in the Murray-Darling Basin, South-Eastern Australia. *Australian Journal of Marine and Freshwater Research*, *41*(5)*,* 581-601.

Oubelkheir, K.J., Claustre, H., Sciandra, A. & Babin, M. (2005). Bio-Optical and Biogeochemical Properties of Different Trophic Regimes in Oceanic Waters. *Limnology and Oceanography*, *50*(6)*,* 1795-1809.

Pages, J. & Gadel, F. (1990). Dissolved Organic-Matter and Uv Absorption in a Tropical Hyperhaline Estuary. *Science of the Total Environment*, *99*(1-2)*,* 173-204.

Pierson, D. & Strömbäck, N. (2000). A modelling approach to evaluate preliminary remote sensing algorithms: Use of water quality data from Swedish great lakes. *Geophysica*, *36*(1-2)*,* 177-202.

Preisendorfer, R.W. (1976). *Hydrologic optics*. Honolulu, Hawaii: U.S. Department of Commerce.

Reinart, A., Arst, H. & Pierson, D.C. (2005). Optical Properties and Light Climate in Lake Verevi. *Hydrobiologia*, *547,* 41-49.

Roesler, C.S., Perry, M.J. & Carder, K.L. (1989). Modeling in situ phytoplankton absorption from total absorption spectra in productive inland marine waters. *Limnology and Oceanography*, *34*(8 (Hydrologic Optics))*,* 1510-1523.

Simis, S.G.H., Peters, S.W.M. & Gons, H.J. (2005). Remote Sensing of the Cyanobacterial Pigment Phycocyanin in Turbid Inland Water. *Limnology and Oceanography*, *50*(1)*,* 237-245.

Summers, R.S., Cornel, P.K. & Roberts, P.V. (1987). Molecular size distribution and spectroscopic characterization of humic substances. *Science of the Total Environment*, *62,* 27-37.

Tassan, S. & Ferrari, G.M. (2003). Variability of Light Absorption by Aquatic Particles in the Near-Infrared Spectral Region. *Applied Optics*, *42*(24)*,* 4802-4810.

Tassan, S. & Ferrari, G.M. (1995). An alternative approach to absorption measurements of aquatic particles retained on filters. *Limnology and Oceanography*, *40*(8)*,* 1358-1368.

Weidemann, A.D. & Bannister, T.T. Absorption and Scattering Coefficients in Irondequoit Bay. Limnology and Oceanography 31[3], 567-583. 1986.

Weidemann, A.D., Bannister, T.T., Effler, S.W. & Johnson, D.L. Particulate and Optical Properties During CaCO3 Precipitation in Otisco Lake. Limnology and Oceanography 30[5], 1078-1083. 1985.

Welschmeyer, N.A. (1994). Fluorometric analysis of chlorophyll a in the presence of chlorophyll b and pheopigments. *Limnology and Oceanography*, *39*(8)*,* 1985-1992.

Yacobi, Y.Z.A.J.J., Takács, M. & McElvaine, M. (2003). Absorption spectroscopy of colored dissolved organic carbon in Georgia (USA) rivers: the impact of molecular size distribution. *Journal of Limnology*, *62*(1)*,* 41-46.